

## Tunable hybridization between electronic states of graphene and a metal surface

Alexander Grüneis<sup>1</sup> and Denis V. Vyalikh<sup>2</sup><sup>1</sup>*IFW Dresden, P.O. Box 270116, D-01171 Dresden, Germany*<sup>2</sup>*Institut für Festkörperphysik, TU Dresden, Mommsenstrasse 13, D-01069 Dresden, Germany*

(Received 26 March 2008; published 7 May 2008)

We present an approach to monitor and control the strength of the hybridization between electronic states of graphene and metal surfaces. Inspecting the distribution of the  $\pi$  band in a high-quality graphene layer synthesized on Ni(111) by angle-resolved photoemission, we observe a new “kink” feature that indicates a strong hybridization between the  $\pi$  and the  $d$  states of graphene and nickel, respectively. Upon deposition and gradual intercalation of potassium atoms into the graphene/Ni(111) interface, the kink feature becomes less pronounced, pointing at potassium mediated attenuation of the interaction between the graphene and the substrate.

DOI: [10.1103/PhysRevB.77.193401](https://doi.org/10.1103/PhysRevB.77.193401)

PACS number(s): 79.60.-i, 71.20.Tx, 73.20.-r, 73.63.Fg

Since the discovery of two-dimensional metastable graphene sheets,<sup>1</sup> much research has been devoted to explore its electronic properties because it is most suitable for nano-electronic devices with high electronic mobilities of  $15000 \text{ cm}^2 \text{ V}^{-1} \text{ s}^{-1}$  at room temperature<sup>2</sup> and can be successfully lithographically patterned.<sup>3</sup> The electronic structure of isolated graphene in the vicinity of the Fermi level ( $E_F$ ) is that of a zero-gap semiconductor, wherein the bare bands are linear and the density of states at  $E_F$  equals zero. These exotic properties give rise to a number of fascinating effects, such as quasirelativistic Klein tunneling,<sup>4</sup> an anomalous quantum Hall effect,<sup>2</sup> and a node in the optical absorption close to  $E_F$ .<sup>5</sup> Strong renormalizations of the quasiparticle bands due to electron-electron,<sup>6</sup> electron-phonon,<sup>7</sup> and electron-plasmon<sup>8</sup> interactions were observed by angle-resolved photoemission (ARPES) in pristine graphite and graphene on SiC. The ARPES spectra of graphite single crystals are not affected by substrate (sample holder) interactions since they exceed  $\sim 100 \text{ }\mu\text{m}$  in thickness. With the graphene layer, however, the SiC substrate interacts and transfers electrons to the  $\pi^*$  band of graphene. This charge transfer occurs according to a rigid band shift model since there is no hybridization of the Si and the C orbitals.

The situation is dramatically changed in the case of graphene/metal systems. The strong hybridization of the electronic states and charge transfer between graphene and the metal substrate modify the band structure of graphene. In this respect, intercalation of foreign atoms into those systems is a key point, which can help to understand and separate these two competing phenomena. It has already been demonstrated that graphene epitaxially grown on Ni(111) (Refs. 9 and 10) has an electronic structure quite different to pristine graphene for two reasons. First, the Ni  $3d_{3z^2-r^2}$  and C  $2p_z$  orbitals are elongated along the direction perpendicular to the graphene sheet and have a large overlap. Second, the interplane distance between the graphene layer and the Ni(111) surface is significantly smaller than in bulk graphite. Low energy electron diffraction (LEED) measurements carried out on graphene/Ni(111) system suggest that one atom of the graphene unit cell is located above the topmost Ni layer and the other carbon atom is located on top of hollow sites.<sup>11</sup> This structural assignment is consistent with the observation of a gap opening at the  $K$  point (or Dirac point) at the Brillouin zone (BZ) corner,<sup>10</sup> which indicates that the two

atoms in the unit cell are situated at nonequivalent positions on the Ni(111) surface. Also, it was experimentally found that the K atoms deposited onto the graphene surface penetrate to the graphene/Ni(111) interface already at room temperature.<sup>10</sup> This approach offers an appealing possibility to control the degree of hybridization between the Ni  $3d_{3z^2-r^2}$  and C  $2p_z$  orbitals, which is quite important and strongly motivated by requirements of precise control and functionalization of graphene based nanostructures. Although a few works<sup>10,12</sup> have been conducted with the aim to study modifications of the electronic structure of graphene on metallic substrates, the detailed description of the hybridization phenomena in graphene/metal interfaces is still lacking. Exploiting this effect, however, allows us to explore the charge transfer in the crossover regime between hybridization and the simple rigid band model.

In this contribution, we present a comprehensive and systematic ARPES study of the evolution of the electronic band structure of a graphene monolayer on Ni(111) under gradual penetration of K atoms to the graphene/Ni(111) interface. We show that due to the strong hybridization of graphene and nickel states, the  $\pi$  band is pushed downward by the Ni  $3d$  bands, revealing a new “kink” feature. However, upon gradual deposition of K atoms, the kinklike structure becomes less pronounced, indicating K-mediated attenuation of the hybridization between the graphene and the metallic substrate. In order to quantitatively describe the changes in the electronic structure, we perform calculations on the tight-binding (TB) level. The experiments were performed by using a photoemission spectrometer equipped with a Scienta SES-200 hemispherical electron-energy analyzer, a high-flux He-resonance lamp (Gammadata VUV-5010) in combination with a grating monochromator, and an x-ray source. All valence PE spectra were acquired at a photon energy of  $h\nu = 40.8 \text{ eV}$  (He II $\alpha$ ) with an angular resolution of  $0.3^\circ$  and a total-system energy resolution of  $50 \text{ meV}$ . The samples were measured at room temperature. X-ray photoelectron spectroscopy (XPS) was applied in order to estimate the K  $2p/C 1s$  intensity ratio (K/C) as well as the quality of the samples. The XPS spectra were obtained at a photon energy of  $1486.6 \text{ eV}$  (Al K $\alpha$ ). The cleanliness and high crystalline quality of the prepared structures were cross checked by LEED.

Figures 1(a)–1(c) schematically show the sample prepara-

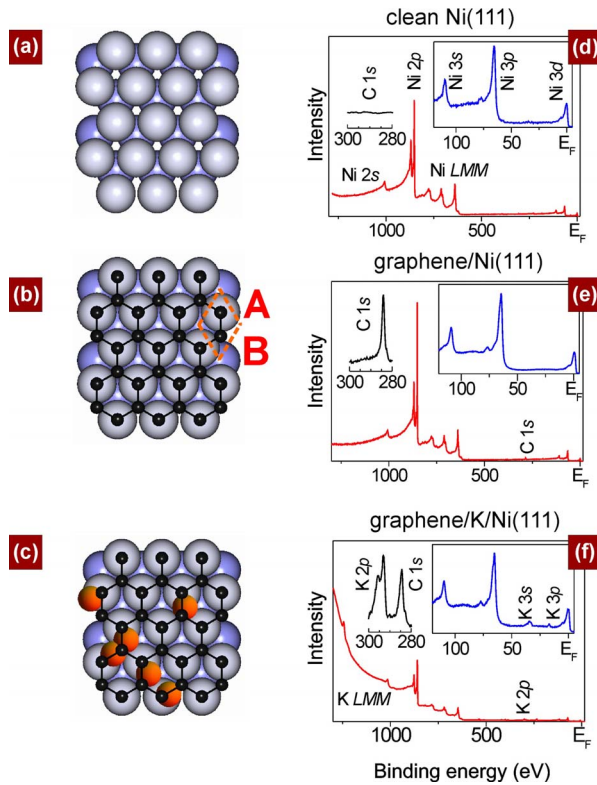


FIG. 1. (Color online) Epitaxial growth and functionalization of a graphene monolayer. (a) Clean Ni(111) surface. (b) Graphene monolayer grown by CVD. The unit cell with the nonequivalent A and B atoms is indicated. (c) Potassium atoms intercalate between the Ni(111) and the graphene. The corresponding XPS spectra for (d) a clean Ni(111) surface, (e) an epitaxially grown graphene monolayer on Ni(111), and (f) a potassium intercalated graphene monolayer with  $K/C=0.69$ .

tion. In the beginning, the electronic and crystalline structures of the clean Ni(111) surface are inspected. Subsequently, we perform chemical vapor deposition (CVD) of propylene in order to grow a graphene layer catalyzed by Ni(111).<sup>10,12</sup> After that, we evaporate potassium onto the sample. Figures 1(d)–1(f) display the XPS spectra taken at each stage of the experiment. After briefly inspecting these spectra, it is obvious that appearance of the graphene layer is accompanied by a sharp peak at  $\sim 285$  eV BE due to electron emission from the 1s core level of carbon.

In Fig. 2, the electronic structure of pristine and potassium doped graphene/Ni(111) is shown. By inspecting the topology of the band dispersions, one can make the following general observations: (i) for  $K/C=0$ , the  $\pi$  band structure is shifted down in binding energy (BE) by  $\sim 2.7$  eV with respect to what is expected from theory for an isolated graphene monolayer; (ii) for  $K/C=0.30$ , the intensity from the Ni 3d states with a flat dispersion close to the Fermi level is suppressed and the  $\pi$  and  $\pi^*$  bands at the K point move up in BE. Thus, for  $K/C=0.30$ , the observed graphene electronic bands are that of a doped graphene layer with a rather small interaction with the Ni substrate. The first point is explained by a strong covalent bonding between the graphene layer and the nickel surface. The second point indicates that intercalated potassium atoms gradually extends the interlayer

distance without affecting the morphology of the graphene monolayer. This decreases the overlap between the wave functions of the C  $2p_z$  and Ni  $3d_{3z^2-r^2}$  states oriented perpendicular to the surface, decreasing the strong interlayer interaction of graphene and the substrate. The proof for intercalation of potassium to the nickel/graphene interface comes from the intensity ratio of the photoemission from the  $\pi$  states of graphene to the  $d$  states of Ni(111). We observe a strong increase in this intensity ratio. This clearly indicates the penetration of potassium atoms into the graphene/nickel interface. Since we do not observe an intercalant band from the potassium 4s, electrons we conclude that we have a complete charge transfer of one electron per potassium atom. The amount of charge transfer is strongly dependent on the carbon material and the intercalant atom, and for different systems one might expect a different degree of charge transfer.<sup>13</sup>

In order to describe the electronic structure of the intercalated graphene monolayer, we perform TB calculations of the  $\pi$  and  $\sigma$  bands, taking into account nearest neighbor interactions.<sup>14</sup> In order to describe the influence of the Ni(111) surface and intercalated K ions on the electronic structure of the graphene monolayer, we adjusted the values of the on-site C  $2p$  energies for the A and B atoms of the graphene unit cell [see Fig. 1(b)], i.e., we employed the rigid band shift model. The  $\pi$  band Hamilton and overlap matrices are given by

$$H(\mathbf{k}) = \begin{pmatrix} \epsilon_{2p} & \gamma_0 f(\mathbf{k}) \\ \gamma_0 f^*(\mathbf{k}) & \epsilon_{2p} + \Delta \end{pmatrix} \quad (1)$$

and

$$S(\mathbf{k}) = \begin{pmatrix} 1 & sf(\mathbf{k}) \\ sf^*(\mathbf{k}) & 1 \end{pmatrix}, \quad (2)$$

respectively. The sum of the phase factors to the three nearest neighbor atoms is given by

$$f(\mathbf{k}) = \exp\left(i\frac{k_x a}{\sqrt{3}}\right) + 2 \exp\left(-i\frac{k_x a}{2\sqrt{3}}\right) \cos\left(\frac{k_y a}{2}\right). \quad (3)$$

At the K point of the two-dimensional Brillouin zone of graphene, we obtain  $f(\mathbf{K})=0$ ; thus, the eigenvalues at K are given by the diagonal elements of  $H(\mathbf{k})$ , i.e.,  $\epsilon_{2p}$  and  $\epsilon_{2p} + \Delta$ , respectively. The electronic band structure is given by solving the Eigenvalue equation  $H(\mathbf{k})\mathbf{c}(\mathbf{k})=E(\mathbf{k})S(\mathbf{k})\mathbf{c}(\mathbf{k})$ , where  $E(\mathbf{k})$  and  $\mathbf{c}(\mathbf{k})$  denote the Eigenvalues and wave function coefficients, respectively. We managed to reproduce the topology of the graphene electronic states by fitting  $\epsilon_{2p}$ ,  $\Delta$ , and the  $\pi$  overlap ( $\gamma_0$ ) to the experimental data. Other parameters related to the  $\sigma$  bands, such as the 2s on-site energy and  $sp$  overlap, need not be changed since the hybridization of the  $\sigma$  states of graphene with the  $d$  states of the Ni(111) surface is rather weak. The values of the parameters used in the TB calculation are summarized in Table I. Our calculations demonstrate that with proceeding potassium intercalation,  $\epsilon_{2p}$  distinctly decreases by 1.2 eV in the direction of  $E_F$ . At the last stage of the experiment, i.e., for complete intercalation,  $\epsilon_{2p}$  was found to be 1.5 eV below  $E_F$ . The values for  $\Delta$  and  $\gamma_0$  do not reveal significant changes with increasing  $K/C$  ratio.

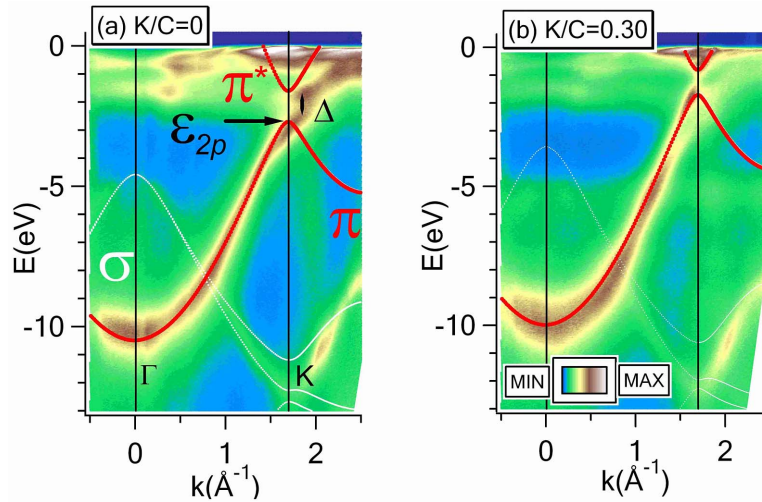


FIG. 2. (Color online) ARPES intensities of the band structure of (a) a pristine graphene monolayer and (b) a doped graphene monolayer. The thick and thin lines denote the TB calculations for the  $\pi$  and  $\sigma$  bands (for the parameters, see Table I). The on-site energy  $\epsilon_{2p}$  and the gap  $\Delta$  are depicted.

Now, let us take a closer look at the shape of the  $\pi$  band between the  $\Gamma$  and  $K$  points shown in Fig. 3. Obviously, in the vicinity of the  $\Gamma$  point, the dispersion of the experimentally derived  $\pi$  band is accurately reproduced by the TB calculation. However, close to the  $K$  point, this agreement is strongly affected by the value of the  $K/C$  ratio. For the case of the pristine graphene/Ni(111) structure ( $K/C=0$ ), the kink shape of this band is clearly visible. The BE of the kink is too high, about 3.5 eV, to attribute it to electron-plasmon or electron-phonon interactions. An accurate consideration of this picture suggests that the  $\pi$  band is pushed downward by the Ni  $3d$  bands. Thus, one can suppose that the kink is a product of hybridization between graphene and nickel states.

Details of the dispersion of the  $\pi$  band close to the point where the kink was monitored for  $K/C=0$  are shown in Fig. 3 as a function of the  $K/C$  ratio. Note that with increasing amount of intercalated potassium atoms, the strength of the kink is gradually reduced. For the case of  $K/C=0.3$ , one can distinguish a second component of the  $\pi$  band. This fact may be interpreted as follows: There are certain sample positions where potassium already intercalates underneath the graphene, reducing its interaction with the Ni(111) surface. Thus, at this stage both phases, a strongly hybridized and an intercalated graphene layer with a small substrate interaction, coexist. For the case  $K/C=0.69$  the kink disappears and the usual step slope behavior of the  $\pi$  band is recovered. A further increase in the  $K/C$  ratio does not reveal significant changes.

TABLE I. Parameters for the on-site energy ( $\epsilon_{2p}$ ), gap ( $\Delta$ ), and nearest neighbor in-plane overlap of C  $2p_z$  orbitals ( $\gamma_0$ ) of the TB calculation shown in Figs. 2 and 3. All values are given in eV.

$K/C$ ratio	0	0.17	0.3	0.69
$\epsilon_{2p}$	-2.7	-2.4	-1.6	-1.5
$\Delta$	0.9	0.8	0.9	0.8
$\gamma_0$	3.2	3.2	3.4	3.3

We discuss now the present experimental and theoretical results. The derived fit parameters for the  $\pi$  bands imply the following physical interpretation: By intercalation of potassium atoms to the graphene/Ni(111) interface, the strong hybridization between the C  $2p_z$  and Ni  $3d_{3z^2-r^2}$  orbitals is weakened. Furthermore, when the graphene layer is lifted up, it is no longer attached to the Ni(111) surface and the lattice constant of graphene might relax to a slightly lower value. These two effects are expected to decrease  $\epsilon_{2p}$  and increase  $\gamma_0$ . While the increase in  $\epsilon_{2p}$  is clearly observable, the increase in  $\gamma_0$  is within the range of the experimental error. The reason for this is probably because the difference in lattice constants is too small (1.42 Å for C–C and 1.44 Å for Ni–Ni) to produce a noticeable change in  $\gamma_0$ . The fact that  $\Delta$  does not change over the whole doping range is quite different to the case of bilayer graphene. In the case of bilayer graphene on SiC, the gap is equal to the doping dependent difference in the on-site energy for the two layers.<sup>15</sup> In the case of a monolayer, the gap is given by the difference between the on-site energies for the  $A$  and  $B$  atoms in the graphene unit cell. Since the  $A$  and  $B$  atoms occupy non-

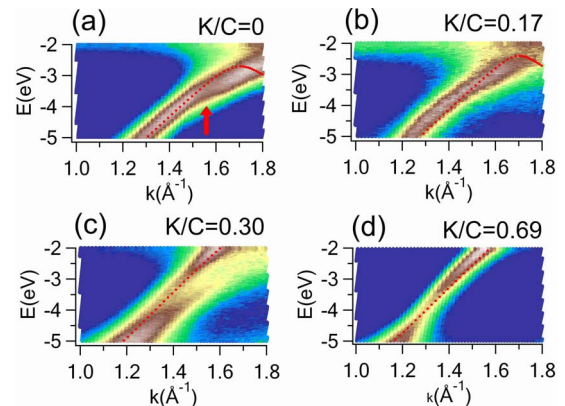


FIG. 3. (Color online) The region of the hybridization kink in the  $\pi$  band of graphene for different doping levels as indicated by the  $K/C$  ratio. The kink is denoted by the arrow in (a). The dots depict the tight-binding calculations.

equivalent sites on the Ni(111) surface [see Fig. 1(b)], this can be easily understood for the case of  $K/C=0$ . For higher doping, the absence of a change in the gap might thus be related to a superstructure of the potassium atoms on the Ni(111) surface. Indeed, a gap opening upon deposition of K on highly oriented pyrolytic graphite was observed.<sup>16</sup>

In order to quantify the charge transfer from potassium, we assume (1) that the whole Ni(111) surface is covered by graphene and (2) that the charge transfer from potassium to the Ni substrate and the graphene is complete. The proofs for these assumptions are (1) that the photoemission intensity does not vary when we move the focus of the He discharge lamp across the sample and (2) that we do not observe a potassium related  $4s$  band at the  $\Gamma$  point. Integration of the density of states above the gap from the bottom of the  $\pi^*$  band up to  $E_F$  (a window of 0.7 eV) leads to a charge transfer of 0.03  $e/C$  atom for  $K/C=0.3$ . Thus, we expect a charge transfer of 0.1  $e/K$  atom to the graphene layer and 0.9  $e/K$  atom to the Ni(111) surface. The large differences between the amounts of charge transfer to graphene and to Ni are attributed to a doping dependent decrease in the electronegativity of the graphene layer.

The  $\pi$  valence bandwidth is given by  $3\gamma_0$  and the experimentally derived values for  $\gamma_0$  in this work are about 20% larger than the values derived from a fit to density functional calculations within the local density approximation (LDA).<sup>6</sup> We thus conclude that the increase in the experimental bandwidth is due to electron-electron correlations, similar to the case of graphite.<sup>6</sup> The valence bandwidth of graphene is not affected by the fact that the graphene monolayer is hybridized with the metal surface since it is identical to the graphite bandwidth. Such a result is surprising since one might expect that the graphene/metal interface enhances the screening of carriers in graphene and, thus, leads to better agreement with the LDA calculations. Hopefully, these new findings will stimulate further theoretical considerations.

Concerning other spectroscopic techniques, it would be

interesting to probe the electronic structure of pristine and functionalized graphene monolayers by optical spectroscopy such as resonance Raman. The (double) resonance Raman process involves  $\pi \rightarrow \pi^*$  transitions,<sup>17</sup> and in order to fulfill the resonance condition, it is clear that the laser energy  $h\nu$  must be larger than  $2|\epsilon_{2p}| - \Delta$ . From the ARPES experiment, we can therefore predict the resonance condition, which yields  $h\nu=4.5$  eV for  $K/C=0$  and  $h\nu=2.2$  eV for  $K/C=1.02$  as a lower limit for the laser energy in resonance Raman measurements.

Finally, we would like to add one more point. It is reasonable to anticipate that alkali-metal intercalated high-quality graphene layers on Ni(111) surfaces bring up the opportunity to use them for the preparation of top quality graphene layers on different substrates. Since the intercalation liberates the graphene from a strong covalent bonding with Ni(111), it would be feasible to peel off intercalated graphene from the substrate.

In summary, we have investigated modifications of the electronic structure of a graphene layer on a Ni(111) substrate upon gradual intercalation of a potassium metal. We found that the hybridization strength between the graphene and Ni states can be successfully monitored by the “hybridization” kink of the  $\pi$  band distribution and the charge transfer from K to graphene follows a rigid band shift model, which is in perfect agreement with the results of TB calculations. We anticipate that the graphene/Ni(111) structure could be successfully used as a model system that is capable of providing valuable insight into the mechanisms of electron correlations and many-body interactions in solids.

A.G. acknowledges a Marie Curie project (COMTRANS). D.V. acknowledges the Deutsche Forschungsgemeinschaft (Grant No. SFB 463) for projects TP B4 and TP B16. Fruitful discussions with Thomas Pichler, Martin Knupfer, Clemens Laubschat, and Serguei Molodtsov are gratefully acknowledged.

<sup>1</sup>A. Geim and K. Novoselov, Nat. Mater. **6**, 183 (2007).

<sup>2</sup>K. S. Novoselov, A. K. Geim, S. V. Morozov, D. Jiang, Y. Zhang, S. V. Dubonos, I. V. Grigorieva, and A. A. Firsov, Science **306**, 666 (2004).

<sup>3</sup>C. Berger, Z. Song, T. Li, X. Li, A. Y. Ogbazghi, R. Feng, Z. Dai, A. N. Marchenkov, E. H. Conrad, P. N. First, and W. A. de Heer, J. Phys. Chem. B **108**, 19912 (2004).

<sup>4</sup>M. I. Katsnelson, K. S. Novoselov, and A. K. Geim, Nat. Phys. **2**, 620 (2006).

<sup>5</sup>A. Grüneis, R. Saito, Ge. G. Samsonidze, T. Kimura, M. A. Pimenta, A. Jorio, A. G. Souza Filho, G. Dresselhaus, and M. S. Dresselhaus, Phys. Rev. B **67**, 165402 (2003).

<sup>6</sup>A. Grüneis, C. Attacalite, T. Pichler, V. Zabolotnyy, H. Shiozawa, S. L. Molodtsov, D. Inosov, A. Koitzsch, M. Knupfer, J. Schiessling, R. Follath, R. Weber, P. Rudolf, L. Wirtz, and A. Rubio, Phys. Rev. Lett. **100**, 037601 (2008).

<sup>7</sup>K. Sugawara, T. Sato, S. Souma, T. Takahashi, and H. Suematsu, Phys. Rev. Lett. **98**, 036801 (2007).

<sup>8</sup>A. Bostwick, T. Ohta, T. Seyller, K. Horn, and E. Rotenberg, Nat. Phys. **3**, 36 (2007).

<sup>9</sup>J. C. Shelton, H. R. Patil, and J. M. Blakely, Surf. Sci. **43**, 433 (1974).

<sup>10</sup>A. Nagashima, N. Tejima, and C. Oshima, Phys. Rev. B **50**, 17487 (1994).

<sup>11</sup>Y. Gamo, A. Nagashima, M. Wakabayashi, and C. Oshima, Surf. Sci. **374**, 61 (1997).

<sup>12</sup>Y. S. Dedkov, A. M. Shikin, V. K. Adamchuk, S. L. Molodtsov, C. Laubschat, A. Bauer, and G. Kaindl, Phys. Rev. B **64**, 035405 (2001).

<sup>13</sup>K. Rytönen, J. Akola, and M. Manninen, Phys. Rev. B **75**, 075401 (2007).

<sup>14</sup>R. Saito, G. Dresselhaus, and M. S. Dresselhaus, *Physical Properties of Carbon Nanotubes* (Imperial College, London, 1998).

<sup>15</sup>T. Ohta, A. Bostwick, T. Seyller, K. Horn, and E. Rotenberg, Science **313**, 951 (2006).

<sup>16</sup>M. Pivetta, F. Patthey, I. Barke, H. Hövel, B. Delley, and W. Schneider, Phys. Rev. B **71**, 165430 (2005).

<sup>17</sup>R. Saito, A. Jorio, A. G. Souza Filho, G. Dresselhaus, M. S. Dresselhaus, and M. A. Pimenta, Phys. Rev. Lett. **88**, 027401 (2001).